A Study on the Effect of Tip–to–Workpiece Distance on Weld Shape in Gas Metal Arc Welding

J. –W. Kim* and S. –J. Na**
(* Laser Application Lab. KRISO, ** Dept. of Prod. Eng. KAIST)

1 INTRODUCTION

Computer simulations of the three–dimensional heat transfer and fluid flow in gas metal arc (GMA) welding have been studied for analyzing the effect of tip–to–workpiece distance on the weld pool shape by considering the three driving forces for weld pool convection, that is the electromagnetic force, the buoyancy force and the surface tension force at the weld pool surface and also by considering the effect of molten electrode droplets. In the numerical simulation, difficulties associated with the irregular shape of the weld bead have been successfully overcome by adopting a boundary–fitted coordinate system that eliminates the analytical complexity at the weld pool and bead surface boundary.

2 FORMULATION

2.1 Governing equations

Figure 1 shows the schematic diagram of the GMA welding process, in which the heat source is moving at a constant speed U and a constant supply of the consumable electrode is maintained through the center of the welding nozzle. The coordinate system (x, y, z) moves with the heat source at the same speed, and its origin coincides with the center of the electrode.

The governing equations, describing the continuity equation, the momentum equation and the energy equation for steady state velocity and temperature fields in the workpiece, may then be written as follows:

$$E_x + F_y + G_z = S \tag{1}$$

where $E = \begin{Bmatrix} \rho u \\ \rho u u - \mu u_x \\ \rho u v - \mu v_x \\ \rho u w - \mu w_x \\ \rho c u T - k T_x \end{Bmatrix}$, $F = \begin{Bmatrix} \rho v \\ \rho v u - \mu u_y \\ \rho v v - \mu v_y \\ \rho v w - \mu w_y \\ \rho c v T - k T_y \end{Bmatrix}$

$G = \begin{Bmatrix} \rho w \\ \rho w u - \mu u_z \\ \rho w v - \mu v_z \\ \rho w w - \mu w_z \\ \rho c w T - k T_z \end{Bmatrix}$ and $S = \begin{Bmatrix} 0 \\ -p_x + f_x \\ -p_y + f_y \\ -p_z + f_z \\ 0 \end{Bmatrix}$

2.2 Boundary conditions

The boundary conditions for the fluid flow and temperature distributions are as follows:

(i) Top surface

$V \cdot n = 0$

$\mu \nabla (V \cdot t_1) \cdot n = -\left(\frac{d\sigma}{dT}\right) \nabla T \cdot t_1$

$\mu \nabla(V \cdot t_2) \cdot n = -(\frac{d\sigma}{dT}) \nabla T \cdot t_2$ in the weld pool,

$u = -U$, $v = w = 0$ in the solid region,

$-k \nabla T \cdot n = q_a(z \cdot n)$ for $r \leq a$

$-k \nabla T \cdot n = q_c = h(T - T_\infty)$ for $r > a$

where z is the unit vector of z-direction and h a combined heat transfer coefficient for the radiative and convective boundary conditions(Ref. 1).

(ii) Bottom surface

$u = -U$, $v = w = 0$

$-k \nabla T \cdot n = q_c$

(iii) Center plane (y=0)

$v = 0$

$\frac{\partial u}{\partial y} = \frac{\partial w}{\partial y} = \frac{\partial T}{\partial y} = 0$

(iv) Side surface

$u = -U$, $v = w = 0$

$-k \nabla T \cdot n = q_c$

(v) Front surface

$u = -U$, $v = w = 0$

$T = T_\infty$

(vi) Rear surface

$u = -U$, $v = w = 0$

$T_b = T_i - (\frac{\partial T}{\partial x})_i \Delta x$

where T_b is the temperature of the boundary and the subscript i means the internal node of the boundary.

2.3 Surface deformation

The weld pool surface under the arc pressure forms a shape which satisfies the equilibrium condition of the surface in the gravitational field. Hence, it is usually convenient to use the condition of equilibrium by directly solving the variational problem subject to the constraint that the volume of weld pool is constant. Ignoring the derivative term of surface tension, the following equation can be derived.

$$\sigma\{\frac{(1+z_y^2)z_{xx} - 2z_x z_y z_{xy} + (1+z_x^2)z_{yy}}{(1+z_x^2+z_y^2)^{3/2}}\} = \rho g z - p_{arc} - \lambda \qquad (2)$$

where the surface tension σ at the weld pool surface was assumed to vary with temperature.

3 NUMERICAL PROCEDURE

Equation (1) is transformed to a general curvilinear coordinate system (ξ, η, ζ), and the grid sizes (i.e., $\Delta\xi$, $\Delta\eta$, and $\Delta\zeta$) are set to be unity to simplify the calculation of transformation coefficients. The second order central differencing technique is used for approximating the diffusion and the source terms. For the convection terms, the hybrid differencing scheme(Ref. 2) is employed. A velocity–pressure correction algorithm SIMPLE–C(Ref. 3) was used for the solution procedure of the discretized equations.

4 CALCULATION RESULTS AND DISCUSSION

For investigating the effect of tip–to–workpiece distance on the weld pool formation, the relevant parameters to the tip–to–workpiece distance variation are selected as shown in Table 2. It was considered from the analysis that the increase of the arc length due to the increased tip–to–workpiece distance makes the distribution of heat, current flux and pressure of arc be expanded(Refs. 4–6).

In the experiment for the tip–to–workpiece distance variation, it was revealed that the effect of tip–to–workpiece distance on the weld shape is considerable(Fig. 2). Figure 3 shows the fluid flow

pattern at the center plane(y = 0*mm*) in the weld pool. As the tip–to–workpiece distance decreases, the decreased radii of welding current flux and distributed velocity of the molten electrode were considered and consequently the maximum velocity of the fluid motion is increased. Figures 4 show the comparisons of the calculated weld shape with experimental one. The calculated penetration shape was underestimated in the condition of 15*mm* tip–to–workpiece distance in comparison with the measured weld shape and slightly overestimated in the condition of 25*mm* tip–to–workpiece distance, which is considered to be due to the rough model of transferred molten droplets. In spite of many assumptions and simplifications, it is revealed that the calculated weld shapes correspond well with those of experiments. It can be thus expected that a better model of molten electrode droplets could make the calculation be more accurate.

5 CONCLUSION

From the experiment and calculation results, it was revealed that the tip–to–workpiece distance exerts a considerable influence on the formation of weld pool and then weld bead shape by affecting the arc length and welding current. The tip–to–workpiece distance is thus considered as one of the important variables which control the formation of the GMA welds.

REFERENCES

1. Goldak, J., Bibby, M., Moore, J., House, R. and Patel, B. 1986. Computer modeling of heat flow in welds. *Metall. Trans.* 17B(9): 587–600
2. Patankar, S. V. 1980. *Numerical Heat Transfer and Fluid Flow.* McGraw–Hill, NewYork
3. Jang, D. S., Jetli, R. and Acharya, S. 1986. Comparison of the PISO, SIMPLER, and SIMPLEC algorithms for the treatment of the pressure–velocity couplingproblems. *Numerical Heat Transfer* 10: 209–228
4. Lin, M. L. and Eagar, T. W. 1986. Pressures produced by gas tungsten arcs. *Metall. Trans.* 17B(9): 601–607
5. Cary, H. B. 1979. *Modern welding technology.* Prentice–Hall Inc., Englewood Cliffs N.J., pp.169–178
6. Tsai, N. S. and Eagar, T. W. 1985. Distribution of the heat and current fluxes in gas tungsten arcs. *Metall. Trans.* 16B(12): 841–846

Table 1 Parameters used in computations

ρ = 7200 Kg/m^3	T_∞ = 20 °C
μ = 0.006 $Kg/m\,s$	T_ℓ = 1520 °C
β ≒ 10^{-4} K^{-1}	T_v = 2500 °C
μ_m = 0.26×10^{-6} H/m	H = 12 mm
$d\sigma/dT$= 10^{-5} N/m °C	U = 7 mm/sec

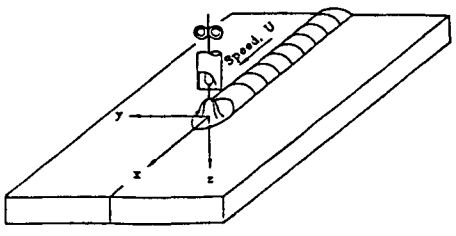

Fig.1 Schematic sketch of GMA welding system

Table 2 Relevant parameters to the tip–to–workpiece distance(L) variation

tip–to–workpiece distance [mm]	a [mm]	b [mm]	c [mm]	e [mm]	P_{max} [KN/m²]	Q [W]
15	8.0	5.2	5.4	1.6	0.85	6615
20	10.0	6.5	6.0	2.0	0.80	6170
25	12.0	7.8	7.2	2.4	0.75	5733

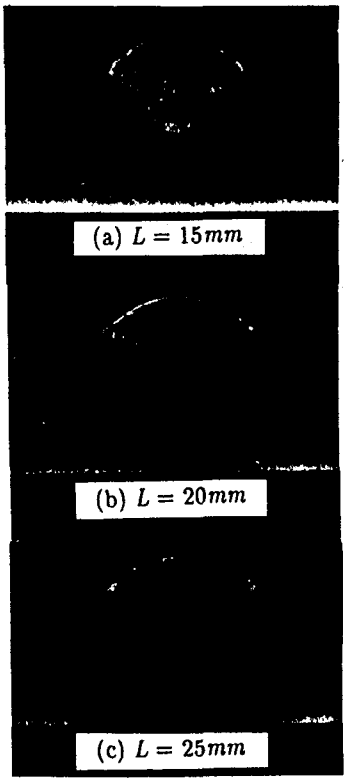

Fig.2 Photographs of weld geometry

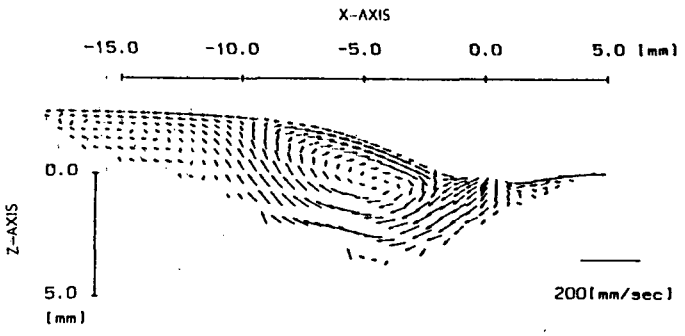

Fig.3 Velocity distribution at the center plane(y = 0mm) in weld pool($L = 20mm$)

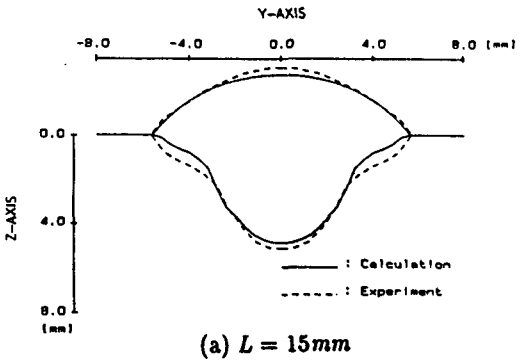

(a) $L = 15mm$

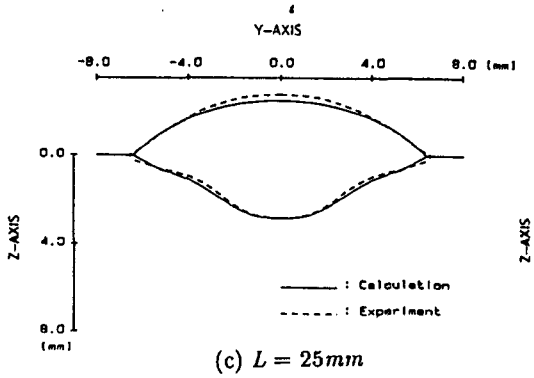

(c) $L = 25mm$

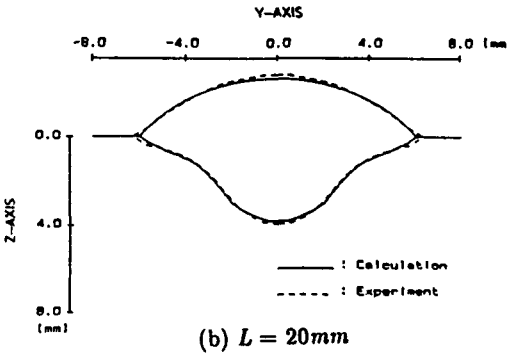

(b) $L = 20mm$

Fig.4 Comparisons of calculated weld shapes with experimental ones